Journal of Biogeography

Biogeography of shell morphology in over-exploited shellfish suggests adaptive tradeoffs on human-inhabited islands and incipient selectively driven lineage bifurcation

Journal:	*Journal of Biogeography*
Manuscript ID	Draft
Manuscript Type:	Research Paper
Date Submitted by the Author:	n/a
Complete List of Authors:	Hamilton, Ashley; Texas A&M University Corpus Christi, Life Sciences Selwyn, Jason; Texas A&M University Corpus Christi, Life Sciences Hamner, Rebecca; Texas A&M University Corpus Christi, Life Sciences Johnson, Hokuala; NOAA Office of Marine National Sanctuaries, Office of Marine National Sanctuaries Brown, Tia; NOAA Office of Marine National Sanctuaries, Office of Marine National Sanctuaries Springer, Shauna; Conservation International - Center for Ocean, Hawaii Program Bird, Christopher; Texas A&M University Corpus Christi, Life Sciences
Key Words:	fisheries-induced evolution, adaptation, adaptive capacity, climate change resilience, phenotypic variation, morphometrics

Biogeography of shell morphology in over-exploited shellfish reveals adaptive tradeoffs on human-inhabited islands and incipient selectively driven lineage bifurcation

Adaptive tradeoffs in shell morphology

Ashley M. Hamilton[1], Jason D. Selwyn[1], Rebecca M. Hamner[1], Hokuala K. Johnson[2], Tia Brown[2], Shauna Kēhaunani Springer[3], and Christopher E. Bird[1]

[1]Department of Life Sciences
Texas A&M University -Corpus Christi
6300 Ocean Drive
Corpus Christi, TX 78411

[2]Papahānaumokuākea Marine National Monument
NOAA Office of Marine National Sanctuaries
1845 Wasp Blvd, Building 176
Honolulu, HI 96818

[3] Conservation International - Center for Ocean, Hawaii Program
3555 Harding Ave Suite 200
Honolulu, HI 96816

cbird@tamucc.edu

ACKNOWLEDGEMENTS

The scientific results and conclusions, as well as any views or opinions expressed herein, are those of the authors and do not necessarily reflect the views of the National Oceanic and Atmospheric Administration (NOAA) or the U.S. Department of Commerce. AMH was funded by the Louis Stokes Alliance for Minority Participation program (NSF-HRD-1304975). This project was funded in part by the following awards: Army Corps of Engineers W9126G-12-2-0066, National Science Foundation MRI-CNS-0821475, and NOAA Saltonstall-Kennedy 15PIRSK23. Papahānaumokuākea Marine National Monument funded the research cruises aboard the RV Searcher (Doc Littenberg, Barbara Littenberg, Capt. Jon Littenberg, Gillian Wysock, Noah Nugent, Capt. Becca Johnston) to collect specimens from the NWHI with the assistance of Patrick Springer, Kanoe Morishige, Randy Kosaki, Makani Gregg, Kane Lind, Keahi Lind, Pekelo Lind, Brenda Bennett, Kaimalino Woo, Mikala Minn, Christopher Holz, Albert Espaniola, Pelika Andrade, Misaki Takabayashi, Dean Tokishi, David Graham, Andy Collins, and the rest of the PMNM intertidal survey participants. Permits PMNM-2011-041, 2012-049, 2014-026, 2015-026 were obtained for collections in PMNM. The Nature Conservancy's Maui Marine Program (Emily Fielding, Roxie Sylva, Karin Osuga, Analea Fink, Alana Yurkanin), Kīpahulu 'Ohana (Leimama Lind-Strausse; Keahi, John, Tweetie, Kaneholani, Isaiah , Zakiah Lind; Roman and Princess Pi'imauna-Beck, Scott Crawford, Stephan Reeve, Rick

Rutiz,), Kalena Center (The Triangle), Nā Mamo O Mūʻolea (Hank Eharis, Walter and Wailena Pu, Claudia Kalaloa, Brian Villiarimo, Barry Villiarimo, Jan Elliott, Kenneth Davis, Janelle Baoy, Ipo Mailou), and the Haleakalā National Park (James Herbaugh and Natalie Gates) provided support and assisted in collecting and processing specimens from Maui. Rob Toonen, Matt Iacchei, Kanoa Severson, Kelly Pennoyer, Lauren Gurski, and Patricia Cockett helped with sample collection on Kauaʻi, Oʻahu, and Hawaiʻi. Aunty Haunani and Sabra Kauka provided transportation and access to Nuʻalolo Kai and Nuʻalolo ʻĀina on Kauaʻi. The United States Kauaʻi Pacific Missile Range Facility provided access and logistical support for additional collections on Kauaʻi. Dr. Steve Gittings performed the NOAA internal review (Section 515 Pre-dissemination Review Documentation and Certification) of this work and provided useful feedback that improved the manuscript. Big mahalos to William Ailā, and Hawaiʻi State Department of Land and Resources for supporting this work.

ABSTRACT

Aim: To identify potentially human-mediated biogeographic patterns in selection and adaptive tradeoffs affecting the evolution an over-exploited shellfish.

Location: Hawaiian Archipelago

Taxon: Mollusca, Gastropoda, Patellagastropoda, Nacellidae, *Cellana exarata,* ʻOpihi makaiauli

Methods: We surveyed phenotypic characters associated with temperature and predation avoidance across the entire species range and tested for differences in the relationship between these characters and latitude, on islands with and without humans.

Results: Among all limpets surveyed, there was a bimodal distribution in shell color (light, dark) and a parapatric pattern of shell coloration across the archipelago with lighter shells being prevalent on the uninhabited islands and darker, more camouflaged shells being prevalent on the inhabited islands. On the cooler, uninhabited islands, all morphometric characters associated with thermal avoidance (surface area, height, and doming) increased with decreasing latitude. On the hotter, inhabited islands, however, shells were flatter, less variable, and less adapted for avoiding thermal stress than predation.

Main Conclusions: The biogeographic patterns in shell phenotype and previous genetic studies suggest that the population is beginning to bifurcate in response to disruptive selection and geographic isolation between the islands with and without humans. Decreased phenotypic and genetic diversity on the inhabited islands despite much larger populations of ʻopihi suggests a prominent historical bottleneck. The prevalence of maladaptive dark, flat phenotypes for thermal avoidance on the inhabited islands suggests that predation is a stronger selective force, driving adaptive tradeoffs in shape and color. We propose that this is likely a case of fisheries-induced evolution and a millennium of harvesting is the most likely selective pressure driving the observed biogeographic patterns in shell morphology. The flatter, darker shells will allow body temperatures to rise higher in direct sunlight, therefore we hypothesize that the thermal niche of ʻopihi is narrower on inhabited islands and will continue to narrow as Earth warms. This study highlights the utility of using intraspecific biogeographic patterns in phenotype to identify adaptive tradeoffs in response to varying selective pressures and identify nascent ecologically driven lineage splitting.

Keywords: fisheries-induced evolution, adaptation, adaptive capacity, climate change resilience, phenotypic variation, morphometrics

1 INTRODUCTION

Variation in the selective landscape can drive the phenotypic structure in populations (Johnson & Barton, 2005); therefore, biogeographical patterns of phenotype can be indicative of variation in underlying selective pressures (Mayr, 1963). Selection acts on phenotypes; consequently, acclimation and adaptation to selective pressures present as changes in the frequency distribution of phenotypes (Belonsky & Kennedy, 1988; Lande & Arnold, 1983). Selective pressures can drive local adaptation (Blondel, 2008; Lind, Ingvarsson, Johansson, Hall, & Johansson, 2011; Guo, DeFaveri, Sotelo, Nair, & Merilä, 2015), population structuring (Schemske, 1984; Bekkevold et al., 2005; DeFaveri, Jonsson, & Merilä, 2013), and even lineage diversification (Shepard & Burbrink, 2011; Pavlova et al., 2013), especially when correlated with gene flow restrictions (Schemske, 1984; Blondel, 2008; Lind et al., 2011). Selection can also affect phenotypic diversity, with both directional and stabilizing selection reducing phenotypic variation (Hoekstra et al., 2001; Lemos, Meiklejohn, Cáceres, & Hartl, 2005). On the other hand, disruptive and balancing selection maintain phenotypic diversity, and spatio-temporal heterogeneity in selective forces can promote increased phenotypic variation (Rainey & Travisano, 1998).

The extent of phenotypic variation and limits on the adaptation of any single phenotype are governed by the effects of adaptive tradeoffs on the overall fitness of an organism (reviewed in Agrawal, Conner, & Rasmann, 2010). A single-trait tradeoff occurs when multiple selective pressures affect a single phenotype, preventing the maximization of fitness in response to any one of the multiple selective pressures. Single-trait tradeoffs can lead to polymorphisms when selective pressures vary in space due to either local adaptation or phenotypic plasticity (Agrawal, Conner, & Rasmann, 2010; Futuyma, 2013). For example, the shell thickness of the intertidal snail *Littorina obtusata* covaries with predation pressure at the expense of body mass and, presumably, physiological maintenance of the organism (Trussell, 2000).

Adaptive tradeoffs and selective landscapes can be influenced by anthropogenic activities, leading to human-induced evolution (Hendry, Gotanda, & Svensson, 2017). For example, anthropogenic activities have indirectly led to a tradeoff in offspring quantity and quality in peacock butterflies (*Aglais io*) where there is increased offspring survival in less impacted landscapes but increased fitness in the few offspring produced in more impacted landscapes (Serruys & Van Dyck, 2014). The direct selective pressures that lead to fisheries- and harvest-induced evolution can have even stronger effects (Heino, Pauli, & Dieckmann, 2015; Kuparinen & Fests-Bianchet, 2017).

Two strong selective pressures that are influenced by humans and vary across biogeographic space are temperature and predation. (1) Temperatures generally increase with decreasing latitudes, increased exposure to solar irradiance, and can drive adaptations to tolerate or avoid stressful conditions, especially in ectotherms (Veryheyen & Stoks, 2018). Temperatures are also increasing in conjunction with rising levels atmospheric carbon dioxide (Snyder 2016), pushing ectotherms closer to their thermal limits (Pinsky, Eikeset, McCauley, Payne & Sunday, 2019). Adaptations in ectotherms enabling thermal regulation and avoidance can be effective in ameliorating thermal stress. For example, ectotherms can seek thermal refuges (Dillon, Liu, Wang, & Huey, 2012) or employ behaviors that modulate temperature (Miller & Denny, 2011; Seuront & Ng, 2016). Morphological features, such as shell size and shape in gastropod snails, can affect the body's heat budget (Denny & Harley, 2006; Harley, Denny, Mach, & Miller 2009), and lighter coloration can decrease the absorbance of solar irradiation which can result in decreased body temperature (Pereboom & Biesmejer 2003; Trullas, van Wyk, & Spotila, 2007; Geen & Johnston, 2014). (2) Predation is often correlated with other habitat and environmental characteristics (Beukers & Jones, 1998), and in edible species, proximity to humans can be an important predictor (Williams et al., 2008; Cinner, Graham, Huchery, & MacNeil, 2013). Adaptations in response to predation include a decrease in mean body size (Ratner & Lande, 2001; Trussell, 2000; Meiri, 2008), increased frequency of protective characters (Leonard, Bertness, & Yund, 1999; Julian Caley & Schulter, 2003; Trussell, 2000), and cryptic coloration (Merilaita et al., 2001, Miller & Denny 2011). For example, mussels have been shown to exhibit an increase in shell strength and more tightly attach to substrate due to predation (Leonard et al., 1999).

In intertidal ectotherms, such as patellogastropods, both predation and thermal stress can be intense (Vermeij, 1973; Lowell, 1984; Branch, Trueman, & Clark, 1985; Knight, 2011). Under thermally stressful conditions which occur during periods of emersion and direct solar irradiance in the middle of the day, lighter-colored, taller shells with greater surface area are advantageous in limiting thermal and desiccation stresses (inferred from Denny & Harley 2006). Lighter colors reflect solar irradiation (Miller & Denny 2011); shells with greater surface area can shed more heat to the atmosphere (Denny & Harley 2006); and taller shells can experience greater wind velocities, aiding in heat dissipation (Harley et al. 2009), while absorbing the same amount of solar irradiation as shorter shells with less surface area (calculated from Pennell & Deignan 1989, see Denny & Harley 2006). Indeed, a pattern of increasing shell height with decreasing latitude was observed in the limpet, *Patella depressa*, on the Iberian peninsula (Hines et al., 2017).

Flatter, cryptically colored shells, however, are advantageous in avoiding predation, setting up a potential tradeoff with morphologies that ameliorate thermal stress (Hines et al., 2017). Predators such as fishes and crabs cannot prey as efficiently on flatter-shelled limpets because both crushing the shell apex (Lowell, 1986; Vermeij, 1993) and applying lateral force for dislodgement is more difficult. Cryptically-colored shells that blend into the background are also more difficult for predators to detect (Miller & Denny 2011) and is an important mechanism

of survival for intertidal gastropods (Manríquez, Lagos, Jara, & Castilla, 2009). Sorenson and Lindberg (1991) concluded that *Lottia pelta* limpets with less cryptic shell coloration were more commonly consumed by American black oyster catchers (*Haematopus bachmani*), and Mercurio, Palmer, and Lowell (1985) employed experimental transplants to demonstrated that cryptic coloration results in lower rates of predation in the limpet, *Collisella digitalis,* by both fishes and birds.

The over-exploited, endemic Hawaiian limpets, *Cellana* spp., provide an ideal opportunity to test for adaptive tradeoffs in shell morphology where thermal stress and predation are negatively correlated. *Cellana exarata,* locally known as ʻopihi makaiauli, ranges along a latitudinal and thermal gradient from Gardner Pinnacles (25°N) to the Big Island of Hawaiʻi (19°N) where the morphology transitions from light-colored and tall-shelled to dark-colored and flatter-shelled (Kay & Shoenberg-Dole, 1991). All of the islands are predominantly composed of dark basaltic substratum, which makes lighter, heat-reflecting shell colors disadvantageous in the face of predation pressure, while darker shells are more camouflaged from predators. In the hotter Main Hawaiian Islands (MHI, Kauaʻi – Hawaiʻi), ʻopihi have been intensely harvested (Kay & Magruder, 1977; McCoy, 2008) ever since they were colonized, A.D. 940-1130 (Athens, Rieth, & Dye, 2014). The uninhabited, cooler Northwestern Hawaiian Islands (NWHI) are subject to lower predation pressure since all but one of these islands (Nihoa) have never been settled by humans (Kikiloi et al., 2017) and they are presently within the Papahānaumokuākea Marine National Monument where harvest by humans is largely illegal. Further, the NWHI harboring ʻopihi are small (<69 hectares) and devoid of terrestrial predators capable of consuming adult ʻopihi such as rats and mongooses.

The Hawaiian archipelago provides ample opportunity for physical and genetic isolation among islands (Toonen et al., 2011), which can foster local adaptation (Blondel, 2008). Indeed, there are gene flow restrictions in *C. exarata* among islands with varying levels of genetic isolation across the archipelago (Bird, Holland, Bowen, & Toonen, 2007; Cockett 2015). Importantly, the most pronounced genetic isolation is found between the uninhabited NWHI and inhabited MHI. Cockett (2015) also found that genomic diversity decreased, on average, from the smaller populations in the NWHI to the larger populations in the MHI, a signature of a historical population bottleneck. Despite these genetic patterns and morphological differences between the NWHI and MHI ʻopihi, genetic investigations have been unable to identify species-level differentiation (Samollow, pers. comm. (allozymes); Reeb, 1995 (mtDNA); Bird, Holland, Bowen, & Toonen, 2011 (mtDNA & nDNA); Cockett, 2015 (RADseq)).

Here we conduct the first rigorous investigation of the biogeography of shell morphology and coloration in *C. exarata* across the entire species range. We test for a decline in morphometric variation from the NWHI to the MHI that parallels the genetic pattern reported by Cockett (2015). We hypothesized that if thermal and desiccation stress were the dominant selective pressures affecting *C. exarata*, then shells would be progressively lighter-colored and taller with greater surface area down the latitudinal gradient. We test this hypothesis on both the inhabited and uninhabited islands to test for a competing effect of predation on the adaptation of

ʻopihi to thermal stress. If predation is the most important selective pressure, then we expect that shells would be flatter and darker, making the ʻopihi more difficult to detect and dislodge from the substratum. We conclude by discussing the observed biogeographic patterns and the potential role of humans in the evolution of ʻopihi.

2 MATERIALS AND METHODS

2.1 Sample Collection and Geographic Metadata

Cellana exarata were collected from eight Hawaiian islands between 2012 and 2016: ʻŌnū (ON, Gardner Pinnacles, Puha honu), Lalo (LA, La Perouse Pinnacles, Mokupāpapa), Mokumanamana (MM, Necker), Nihoa (NI), Kauaʻi (KA), Oʻahu (OA), Maui (MA), and Hawaiʻi (HI, Big Island; Table 1; Kikiloi et al., 2017). The NWHI were accessed during intertidal monitoring cruises sponsored by Papahānaumokuākea Marine National Monument, and eight ʻopihi were collected from each of six, 1 cm size classes. In the MHI, shells of legal harvesting size were haphazardly collected along a 7 km section of coastline on Maui, two locations on Kauaʻi (Miloliʻi and Kekaha) and Oʻahu (Kakaʻako, ʻĀina Moana), and one location on each of the remaining islands. All sites were composed of natural basalt formations with the exceptions of the Oʻahu and Hawaiʻi sites (basalt riprap) and Kekaha (emergent coral reef).

Geographic location information for each sampling site was obtained using Google Earth Pro 7.3.2.5776. The one-dimensional geographic location of each sampling site was defined as the sum of the channel widths at their narrowest point between ʻŌnū and the island of each site (stepping-stone distance, Bird et al., 2007). This is an estimate of isolation, where distance is defined as the minimum distance a larva could travel between two islands, and direct exchange between non-adjacent islands is assumed to be negligible.

2.2 Character State Scoring, Missing Data Imputation, and Allometric Normalization

The newest parts of the shell (rib tips) were used to classify shell color based upon the expression of black periostracum, the proteinaceous shell coating, and irrespective of shell erosion. Rib tip color was scored estimating the percentage of rib tips that had black pigment in increments of 25% in each of four quadrants and averaging the scores for each shell. If >=50% of rib tips were black, the color morphotype of the shell was classified as black. Otherwise the shell was classified as white (Figure 3).

We were primarily interested in investigating morphometric characters related to thermal avoidance: shell surface area and shell height. We measured shell height (H), length (L), and width (W) directly using dial calipers and inferred surface area by modelling the shell as an ellipsoid cone (Table 2). Because the lateral area of a cone does not account for shell doming, we calculated a doming index based upon the lateral length from the apex to posterior margin of the aperture along the axis of symmetry in the shortest distance possible ($L_{1,3}$) and along the curve of shell's surface ($C_{1,3,}$ Figure 2) using ImageJ (Schneider, Rasband, & Eliceiri, 2012) and images

taken from the lateral perspective (see Figure 2). Landmarks defined by cartesian coordinates were placed on either end of a size standard, the apex (Point 1), the anterior (Point 2) and posterior aperture edge (Point 3). The lengths ($L_{1,3}$, $L_{2,3}$) were calculated using the Pythagorean Theorem, while $C_{1,3}$ was determined by drawing a line using the segmented line tool from point 1 to 3 along each shell's edge, and then converted to mm using the size standard. Finally, a scale correction factor to align ImageJ measures with those from the calipers was determined by dividing L_i by $L_{2,3i}$, where i is each individual's identity and was multiplied by $L_{1,3i}$ and $C_{1,3i}$.

Since some shells were missing either length or width data due to shell damage, we imputed the missing data based on the present width or length respectively. The best models between a linear and power function for imputing L from W and vice-versa were identified by satisfying the assumptions of least-squares regression models, minimizing the Akaike Information Criterion (AIC) and testing against the null model using a log-ratio test. Heteroscedasticity was explicitly modeled with an exponential variance structure to make the final models (Table S1, Figure S1).

All morphometric measurements were normalized by the mean shell length to remove the effects of allometry using the following equations:

$$Y = aL^b \quad \text{and} \quad Y_i^* = Y_i\left[\frac{\bar{L}}{L_i}\right]^b,$$

where Y is the size of a character (W, H, $L_{1,3}$, $C_{1,3}$), i is an individual's identity, L is the shell length, $\bar{L}$ is the mean shell length, and a and b are constants (Lleonart, Salat, & Torres, 2000). These relationships were tested as described for the imputations (Table S2). To better satisfy the assumptions of each model, the L and Y were natural log-transformed except in the case of width because all assumptions were met without a transformation (Figure S2). After allometric normalization, all individuals smaller than 25 mm in length were excluded from the study because juveniles tend to have different morphologies from adults due to ontological changes (Vermeij, 1973). From the allometrically-normalized measurements, we calculated the height index, width index, doming index, and modeled the surface area of the shell as the lateral area of an ellipsoid cone (Table 2).

2.3 Morphometric Analysis

All analyses were performed using R v3.5.1 (R Core Team, 2018) and the tidyverse of packages (Wickham, 2017) and, along with the data, can be found on github: https://github.com/jdselwyn/Opihi_Morphology.

For all characters associated with thermal avoidance (i.e. shell surface area, height index and doming index), Bayesian hierarchical regression models were fit to model the relationship between morphology and latitude as well as the relationship between the variation in morphology and the stepping-stone distance to ʻŌnū, between island groups (uninhabited vs. inhabited). To account for the observation that meso- and microhabitat are generally dominant features shaping shell morphology in patellogastropods (Denny, Dowd, Bilir, & Mach, 2011), sites and islands were treated as hierarchical, random effects on the intercept of shell morphology. All morphological metrics were modeled using a Gaussian response distribution

and uninformative priors. Each response variable was fit using four models of increasing complexity (Table 3) which were compared using leave-one-out (loo) and Watanabe-AIC (W-AIC) model weights (Vehtari, Gelman, & Gabry, 2017). The models 1 and 2 only attempted to model the morphological metric of interest while models 3 and 4 additionally modelled the variance in that metric (Table 3). All models were fit using the BRMS implementation of STAN (Gelman, Lee, & Guo, 2015; Bürkner, 2017) with four chains run for 5,000 iterations (1,000 for warm-up). Successful convergence of the chains was assessed using Rhat and visual inspection of traceplots (Vehtari, Gelman, Simpson, Carpenter, & Bürkner, 2019).

Upon confirmation of successful model convergence, the best models were chosen based on model weight (Link & Barker, 2006). Global model effects such as a Bayesian equivalent to r^2 were calculated, and individual model coefficients were assessed to determine pairwise differences among islands. Finally, Bayes factors (*K)*, were used to assess the strength of evidence for the *a priori* hypotheses that there is greater thermal avoidance and variation in the characters associated with thermal avoidance between uninhabited and inhabited islands and that the effect of latitude is greater in uninhabited than inhabited islands. The strength of evidence (*K*) for a hypothesis can be negligible (0-3), positive (3-20), strong (20-150), or very strong (>150; Kass & Raftery, 1995). To classify sites according morphometric character traits and their variation, *post hoc* Tukey contrasts were performed among sites with pairs being defined as different if the difference between the posterior means of a given pair did not contain 0 within the 95% credible interval. Groupings were labeled alphabetically from highest values on the y-axis (a) to lowest (z).

3 RESULTS

A total of 402 shells were collected and measured (Table 1). A few shells (3.2%) were missing measurements of *L* or *W* due to shell damage. The allometric power model better described the relationship between *L* and *W* than a linear model and was used for imputing missing values from damaged shells (Table S1, Figure S1). When normalizing shell measurements for allometry, all of the shells were well described by one allometric relationship for each shell character (*W, H,* $L_{1,3}$*,* $C_{1,3}$) and the mean length to which all measurements were normalized was 37 mm (Table S2, Figure S2).

There was a bimodal distribution of shell color, where 86% of shells exhibited either <10% or >90% black rib tips (Figure 3). The color morphotypes exhibited a parapatric distribution, with overlap of the two color morphotypes occurring primarily on the central islands (MM, NI, KA; Figures 1 & 3, Table 1), a predominance of white morphotypes on the two most northwestern islands (ON and LA), and a predominance of the black morphotype on the three most southeastern islands (OA, MA, and HI). On Kaua‘i, there were more white morphs at the site with a calcium carbonate shoreline (29% white, KA2, Table 1), than at the site with a basaltic shoreline (6% white, KA1).

The best models of the relationships between the morphometric characters associated with thermal avoidance, their variance, latitude, and location were all Full + σ_b and explained 31-42%, 50-58% and 37-52% of the variance in surface area, height, and doming, respectively (Table 4, Figures 4 & 5).

'Opihi on the uninhabited NWHI islands had significantly taller ($K = 72$, $p_{posterior} = 0.99$) and more domed shells ($K = 46$, $p_{posterior} = 0.98$) with greater surface areas ($K = 56$, $p_{posterior} = 0.98$) despite residing at higher latitudes (Figure 4, Table S3). The differences in surface area were primarily governed by differences in height, with 5x more range in height index than width index (Figure 6). Additionally, the morphometric indices associated with thermal avoidance (shell surface area, height index, and doming index) had different relationships with latitude on uninhabited versus inhabited islands (respectively, $K = 17, 17, 18$ and $p_{posterior} = 0.94, 0.94, 0.95$; Table S3). Specifically, on uninhabited islands, surface area, height, and doming increased as latitude decreased with a posterior probability of a positive slope being between 0.92 and 0.96 (Table 5), but there was either no significant relationship or a negative relationship with latitude on the inhabited islands with 65-85% posterior probability of the slopes being negative. The estimated changes in surface area, doming, and height per degree decrease in latitude on the uninhabited islands were 1.2 cm^2, 0.014, and 0.030, respectively. On the inhabited islands, there was some support for a slight decrease in the doming index and height index of -0.0046 and -0.016 per degree of latitude, respectively. The slight decreases in all three morphometric character traits in the MHI were due to Kaua'i having significantly taller, more domed shells with greater surface area than the other three islands (Figure 4). The morphometric characters did not significantly differ between sites within islands (KA1, KA2; OA1, OA2; Figure 4).

'Opihi on the uninhabited NWHI islands had significantly more variation in shell surface area ($K = 4.5$, $p_{posterior} = 0.82$), height ($K = 729$, $p_{posterior} = 1.0$), and doming ($K = 4166$, $p_{posterior} = 1.0$; Figure 5, Table S3). There was a significant difference in the relationship between the variation in shell doming and location on the inhabited and uninhabited islands ($K = 21$, $p_{posterior} = 0.96$; Table S3), with 97% posterior probability of a positive in the NWHI and 89% posterior probability of the slope being negative in the MHI (Table 5). While there were not significant differences in the relationships of surface area and height with location between inhabited and uninhabited islands, there was a trend of decreasing variation in shell height with increasing distance from the uninhabited islands, with 76% posterior probability of a negative slope. There were no significant differences in the variation in shell characters between sites within the same islands (Figure 5).

4 DISCUSSION

4.1 Incipient Lineage Bifurcation

Together, the parapatric and bimodal distribution of shell coloration (Figures 1, 3) and the disjunct pattern of shell shape (Figure 5) are indicative lineage bifurcation. Bimodally distributed phenotypes exhibiting a parapatric pattern are classic indicators of disruptive selection and

partial reproductive isolation (Gauthier, Lumaret, & Bédécarrats, 1998; Futuyma, 2013). Gene flow estimates between the NWHI and MHI sites (0.02 - 0.77 migrants per generation, mtDNA, Bird et al., 2007) as well as estimates of population genetic structure ($F_{CT} \sim 0.16$, RADseq, Cockett, 2015) support this hypothesis, as do studies from additional species and passive larval simulations which identify a gene flow restriction somewhere between Kauaʻi and Mokumanamana (Toonen et al., 2011; Wren, Kobayashi, Jia, & Toonen, 2016). In contrast to the population genetic analyses, a phylogenetic analysis of both mtDNA (12S, 16S, COI) and nDNA (atpsβ, H3) found no indications of lineage bifurcation in *C. exarata* (Bird et al., 2011). For comparison, the sibling taxon, *C. talcosa*, exhibited a one bp fixed difference in cytochrome C oxidase I between Kauaʻi and the other MHI which was dated to ~2000 ya (Bird et al., 2011). In *C. exarata*, there either has not been enough time for the genetic lineages to sort, or gene flow is sufficient to prevent lineage sorting. The greater shell surface area and height on Kauaʻi relative to the other MHI (Figure 4) may be driven by ongoing gene flow from the NWHI. Overall, the available data support that *C. exarata* is in the early stages of lineage bifurcation. Given our nascent understanding of the processes driving speciation in tropical marine organisms (Bowen, Rocha, Toonen, & Karl, 2013), Hawaiian *Cellana* could serve as a broadly relevant exemplar for broadcast-spawners.

4.2 Reduced Morphometric Variance on Inhabited Islands: Selection or Bottleneck?

The pattern of depressed morphometric variation on the inhabited MHI is consistent with increased directional selection on morphology and/or a population bottleneck. There appears to be strong selection for flatter shells on the inhabited islands, and this may constrain phenotypic variation in the shell surface area and height index. The phenotypes of limpets and other slow-moving intertidal ectotherms are known to be plastic (Kemp & Bertness, 1984; Trussell, 1996; Teske, Barker, & McQuaid, 2007), and there are typically greater differences across microgeographic rather than latitudinal scales (Denny et al., 2011; Seabra, Wethey, Santos, & Lima, 2011;Lathlean, McWilliam, Ayre, & Minchinton, 2015). At least some proportion of the variation in morphology within and between sites is likely due to plasticity. However, the observed depressed morphometric variation on inhabited islands is unlikely to be due to plasticity because we see no likely stimulus to trigger differential gene expression resulting in the population being more uniformly flat and dark on inhabited islands. Another explanation which does not involve selection and has much more evidentiary support is a population bottleneck.

Based upon a genome-wide survey of ~21k SNPs, *C. exarata* exhibited greater genomic diversity on Nihoa (~4.7 km of linear habitat) than on any of the MHI (109-407 km of linear habitat, i.e. larger populations), suggesting that the MHI populations had all experienced a severe bottleneck (Cockett, 2015). The morphometric data presented here exhibit a similar pattern, and therefore it is possible that reduced genetic variation in the MHI is at least partially due to a historical bottleneck. However, population bottlenecks do not necessarily reduce the capacity to respond to selective pressures (Bryant & Meffert, 1993), especially given the plasticity of limpet shell shape in response to environmental conditions (Teske et al., 2007). To decipher between

the effects of genetic variation and selection on the observed patterns in phenotypic variation, it would be necessary to identify and interrogate quantitative trait loci (Wadgymar et al., 2017). Nonetheless, there are inferences that can be made about the role of selection on the observed phenotypes based upon the available data.

4.3 Adaptive Tradeoff: Thermal Regulation and Predation Avoidance

We propose that the pattern of tall, light-colored shells on higher latitude, uninhabited islands and flat, dark-colored shells on lower latitude, inhabited islands is caused by an adaptive tradeoff between thermal and predation avoidance. In response to increasing thermal stress, shells were expected to have greater surface area and be taller, which was observed with decreasing latitudes on the uninhabited islands, consistent with the Iberian limpet *Patella depressa* (Hines et al., 2017). However, darker shells which increase the absorbance of solar irradiation, and thus body temperature (Miller & Denny, 2011), became more prevalent with decreasing latitude on both the uninhabited and inhabited islands. The substratum upon which *C. exarata* resides is mostly dark basalt across its range, and thus darker shells were more camouflaged (except on the emergent coral reef at Kekaha, Kaua‘i), suggesting an adaptation to visual predators (Merilaita, Scott-Samuel, & Cuthill, 2017). In contrast to color which changes gradually, shells abruptly become flatter on the inhabited islands, and while they cannot dissipate as much heat, it is more difficult and less efficient to apply lateral force that would dislodge or crush these flatter shells (Denny, 2000). We propose that the shells on inhabited islands are colored and shaped to avoid detection and dislodgement by predators at the expense of thermal avoidance.

Drilling deeper, the shell morphometric patterns are consistent with both the homogenizing effects of gene flow from the uninhabited islands and selection. As mentioned above, gene flow from the tall-shelled Nihoa population may be opposing selection against tall shells on Kaua‘i, explaining why the ‘opihi on Kaua‘i are intermediate in height, surface area, and doming between the uninhabited island of Nihoa to the northwest and the densely-populated island of O‘ahu to the southeast. In genetic swamping (Duputié, Massol, Chuine, Kirkpatrick, & Ronce, 2012). geneflow overwhelms selection, but here, it seems gene flow is weak enough and selection is strong enough prevent swamping and potentially limit connectivity further. Identifying the source of selection in the MHI and how it relates to human-inhabitance could help to illuminate the dynamics at play.

4.4 Is Human Harvesting Driving the Adaptive Tradeoff?

We are compelled by the available evidence to propose that in the past 900-1100 years (~900-2200 generations for *C. exarata*; see Kay & Magruder, 1977) selective pressures applied by humans in the MHI may have driven the distinct biogeographic patterns in the morphology of *C. exarata* reported here, but more investigation is necessary to make a definitive conclusion. ‘Opihi are intensely harvested today (Tom, 2011) and anthropologic studies show that ‘opihi are a consistent staple of the Hawaiian diet (e.g., McCoy, 2008; McCoy & Nees, 2013). At an

archaeological site on Moloka‘i where *Cellana* spp. were identified to species, *C. exarata* made up 15-60% of the shells (Rogers & Weisler, 2019). White, tall shells on black rocks are certainly easier to spot than dark, flat shells, especially on heterogeneous shores with shaded crevices, and thus there would be a selective advantage to being less conspicuous. While we have been unable to uncover details on how ‘opihi were harvested prior to European contact, it is possible that taller shells were easier to dislodge and may have been and continue to be favored over flatter shells. Harvest pressure by humans was likely to have been highest in the MHI where the vast majority of the population resided. In the NWHI, only Nihoa was settled by a small number of humans (Emory, 1928). A lack of drinking water would preclude settlement further to the northwest, but Mokumanamana was visited. Since 1815, the entire Hawaiian population has resided in the MHI (Kikiloi et al., 2017). If human colonization of the Hawaiian archipelago is driving the observed adaptive tradeoff in *C. exarata*, then we expect that shells from archaeological sites will become taller with greater surface area with age.

Alternative predators from the terrestrial realm are birds, rats, and mongoose. There are three extant bird species that might prey upon ‘opihi (*Numenius tahitiensis*, *Tringa incana,* and *Arenaria interpres*). They have small bills that are generalized for harvesting smaller invertebrates than adult ‘opihi (Dann, 2005; Bent 1929; Marshall 1980). *Arenaria interpres* has been documented to prey upon limpets but they are not abundant (Whitfield, 1985). Further, none of the extinct birds in the current fossil record seem capable of preying upon limpets (see Olson & James, 1982; James & Burney, 1997). The Pacific rat, *Rattus exulans*, was introduced by the Polynesians (Athens, Rieth, & Dye, 2014) and the Europeans later brought *Rattus rattus* and *Rattus norvegicus* as early as 1778 (Matisoo-Smith et al., 1998). While the Pacific rat has had the longest opportunity to affect the ‘opihi populations, we have only observed rats in ‘opihi habitat at one location in 20 years. The mongoose, *Herpestes javanicus*, has been observed in ‘opihi habitat on numerous occasions (CEB, pers. obs.), but was not introduced to Hawai’i until 1883 to control rats (Hays & Conant, 2007). While the distribution of these introduced predators on the inhabited MHI correlates with the biogeographic patterns in ‘opihi morphology, there have only been ~150-250 years since their arrival, and there is no modern record of a drastic change in the morphology of *C. exarata*.

For the remaining visual marine predators (octopi, fish, and crabs), there does not seem to be a correlation between their abundance and the morphology of ‘opihi. *Cellana exarata* generally resides above the grasp of fishes’ jaws (Bird. Franklin, Smith, & Toonen, 2013) and contemporary fish concentrations are higher in the NWHI than the MHI due to decreased fishing pressure (Friedlander & DeMartini, 2002). The only intertidal octopus in Hawai‘i, *Octopus oliveri*, has been commonly observed on intertidal community surveys of Nihoa and Mokumanamana in the uninhabited NWHI (CEB pers. obs.) as well as in the MHI, and the same is the case with crabs.

An alternative hypothesis is that the taller mountains in the MHI cause more cloud cover, decreasing solar irradiance, and thermal stress thereby reducing selection against flatter shells. However, we find it unlikely that increased cloud cover would strongly select for darker shells

and against taller shells with greater surface area. Additionally, the same calm weather conditions that result in thermal stress events for *C. exarata*, which resides above the high tide line and depends on waves for immersion (Bird et al., 2013) and cooling, also result in reduced cloud formation above the high islands (Whiteman, 2000).

4.5 Implications for Management: Thermal Niche

Cellana spp. are over-exploited and the biogeographic pattern described here indicates that most of the population, which resides in the MHI, are being further constrained by evolutionary forces. We expect that in the NWHI, *C. exarata* inhabits hotter microhabitats, and in the MHI, the population is more dependent upon thermal refugia. The thermal niche breadth of *C. exarata* conferred by shell morphology is narrower in the MHI which likely results in reduced habitat exploitation and population size, especially as Earth warms in the tropics (Payne & Smith, 2017). Increasing air temperatures associated with global warming can further constrain the thermal niche. Physiological acclimation (Pintor, Schwarzkopf, & Krockenberger, 2016) or adaptations that increase thermal tolerance could counteract the increased body temperatures caused by flatter shells and warming climate, but the vertical extent of *C. exarata* is presumably limited by its thermal tolerance (Somero, 2002), leaving little room for additional tolerance in the gene pool. Further, acclimation is unlikely to buffer the additional stress from global warming (Gunderson & Stillman, 2015) and could be investigated in this system where thermal stress increases as latitude decreases. .

Given that human harvesting is affecting ‘opihi populations and may be contributing to the flatter morphology, it is possible that harvest regulations could alter present selective pressures. More research is required to link harvesting and flat shells, but if there is a causal link, then encouraging or regulating harvest based upon shell height could allow taller morphotypes to proliferate.

4.6 Conclusions

While testing for biogeographic patterns in genotype is a typical practice among molecular ecologists, there is still much to be learned from patterns in phenotype and, ideally, investigations of biogeography should employ both. We tested for biogeographic patterns in the morphology of shells in an intertidal ectotherm and found distinct biogeographic patterns in adaptations to predation and temperature, signifying an adaptive tradeoff. These patterns in phenotype illuminated previous population and phylogenetic studies and have helped to identify a population in the early stages of splitting in response to partial isolation and disruptive selection. *Cellana* are among the only marine species to have diversified in the Hawaiian archipelago (Bird et al., 2011), and this study identifies one mechanism by which diversification has occurred: parapatry and ecological diversification. We also identified a potential unintended evolutionary consequence of exploitation that negatively affects the long-term sustainability of the fishery by reducing the breadth of a niche dimension . Consequently, knowledge of evolutionary processes is necessary for effective resource conservation and management.

Table 1. Summary of sampling locations and sample sizes (n). The number of black shells (n_{blk}), white shells (n_{wht}), and shells requiring the imputation of either legth or width (n_{imp}) are also listed. NWHI is northwestern Hawaiian islands and MHI is main Hawaiian islands.

Region	Island	Code	Site	Dates of Human Habitation (A.D.) *	Substratum	Year of Collection	n	n_{blk}	n_{wht}	n_{imp}
NWHI	ʻŌnū	ON	Nui	N	Basalt	2016	30	0	30	1
	Lalo	LA	Nui	N	Basalt	2016	21	3	18	0
	Mokumanamana	MM	West Cove	N	Basalt	2012	79	33	46	2
	Nihoa	NI	Adams Bay	1400-1815	Basalt	2013	49	38	11	3
	Subtotal						**179**	**74**	**105**	**6**
MHI	Kauaʻi	KA1	Miloli'i	940-Present	Basalt	2013	33	31	2	4
		KA2	Kekaha	940-Present	$CaCO_3$	2013	65	46	19	6
	Oʻahu	OA1	Kaka'ako	940-Present	Basalt	2013	23	23	0	3
		OA2	Aina Moana	940-Present	Basalt	2013	29	28	1	3
	Maui	MA	Hāna	940-Present	Basalt	2014	26	26	0	1
	Hawai'i	HI	Hilo	940-Present	Basalt	2013	47	47	0	3
	Subtotal						**190**	**170**	**20**	**16**
Total							**402**	**275**	**127**	**26**

*Athens, Rieth, & Dye, 2014; Kikiloi et al., 2017

Table 2. Formulas used to calculate shell indices and estimate surface area. See Figure 2 for descriptions of the measurement variables.

Characters	Formula
Shell Apex Height Index	$H_{ai} = \frac{H}{L}$
Shell Aperture Width Index	$W_{ai} = \frac{W}{L}$
Shell Doming Index	$D_i = \frac{C_{1,3}}{L_{1,3}}$
Shell Surface Area*	$A_s \cong \frac{1}{2}\int_0^{2\pi} \sqrt{L^2W^2H^2\left[L^2\sin^2(t) + W^2\cos^2(t)\right]}\, dt$

* modelled as ellipsoid cone

Table 3. Four models were compared to explain the variation in the morphometric characters shell surface area, height index and doming index (y). Model 1 represents no relationship. The additional models tested for the effect of human presence, latitude, their interaction, island (random), and site within islands (random) assuming either equal variances (s, Model 2), variances related to island and site (Model 3), or variances related to human presence, geographic isolation (Location), island, and site (Model 4).

Model ID	Model Name	Model Structure
1	Null	y ~ 1 s ~ 1
2	Full	y ~ Humans + Latitude + (Humans * Latitude) + Island + Site(Island) s ~ 1
3	Full + σ_a	y ~ Humans + Latitude + (Humans * Latitude) + Island + Site(Island) s ~ Island + Site(Island)
4	Full + σ_b	y ~ Humans + Latitude + (Humans * Latitude) + Island + Site(Island) s ~ Humans + (Humans * Location) + Island + Site(Island)

Table 4. Model fitting results for surface area, doming index, and height index. loo-ic is the leave one out information criterion, and lower values generally indictate a better fit. The models with the highest weights were considered the best (bold). The 95% credible interval for r^2 is CI_{95} r^2.

Modeled Character	Model Name	loo-ic	loo weights	CI_{95} r^2
Surface Area	Null	1528.5	0	0
	Full	1362.3	0.037	0.30-0.42
	Full + σ_a	1296.1	0	0.31-0.42
	Full + σ_b	**1295.8**	**0.963**	**0.31-0.42**
Doming Index	Null	-1864.4	0	0
	Full	-2107.5	0.037	0.41-0.52
	Full + σ_a	-2208.4	0.189	0.38-0.53
	Full + σ_b	**-2209.1**	**0.775**	**0.37-0.52**
Height Index	Null	-1016.4	0	0
	Full	-1311.2	0	0.49-0.58
	Full + σ_a	-1424.8	0.288	0.50-0.58
	Full + σ_b	**-1425.2**	**0.712**	**0.50-0.58**

Table 5. Summary of slopes modelled for (1) surface area, doming index, and height index versus latitude on uninhabited Northwestern Hawaiian Islands (NWHI) and inhabited Main Hawaiian Islands (MHI), and (2) the variance in these morphometric characters versus geographic location. Bolding indicates slopes with a posterior probability >75% .

Region	Character	Median Slope (Change per Degree)	Upper 95% CI	Lower 95% CI	Posterior Probability of Positive Slope	Posterior Probability of Negative Slope
NWHI	Surface Area (cm2)	1.15E+00	2.53E+00	-2.29E-01	**0.957**	0.0427
	Doming Index	1.45E-02	3.55E-02	-5.57E-03	**0.947**	0.0527
	Height Index	2.97E-02	7.65E-02	-1.88E-02	**0.922**	0.0784
	Variance in Surface Area (cm^2)	-5.22E-05	1.96E-03	-2.04E-03	0.528	0.472
	Variance in Doming Index	-1.15E-03	9.96E-06	-2.36E-03	**0.974**	0.0265
	Variance in Height Index	1.82E-04	1.99E-03	-1.67E-03	0.394	0.606
MHI	Surface Area	-1.62E-01	9.33E-01	-1.21E+00	0.349	0.651
	Doming Index	-4.56E-03	1.19E-02	-2.04E-02	0.218	**0.782**
	Height Index	-1.55E-02	2.19E-02	-5.08E-02	0.147	**0.853**
	Variance in Surface Area (cm^2)	-6.40E-04	4.85E-03	-6.19E-03	0.629	0.371
	Variance in Doming Index	1.55E-03	4.84E-03	-1.74E-03	0.107	**0.893**
	Variance in Height Index	1.32E-03	6.43E-03	-3.72E-03	0.24	**0.76**

FIGURE LEGENDS

Figure 1. Map of Hawaiian Archipelago. Sampling sites are labeled by either the island abbreviation or, when there were multiple sites, the site number (as described in Table 1). The biogeographic range of color morphotypes observed in the samples is represented by the filled ovals (peach – lighter shells, grey – darker shells. A photograph of an example shell of each color morphotype from a ventral and dorsal perspective is shown near the islands typically harboring those morphs.

Figure 2. Diagram of shell measurements and landmarks from lateral and ventral perspectives. The numbers represent Cartesian coordinates obtained from photographs, and the letters represent characters: *L* = length, *W* = width, *C* = distance following the edge of the shell which was generally curvilinear. Solid lines represent measurements made with calipers, and dashed lines represent measurements made using photographs.

Figure 3. Histogram of the number of shells that had a given percentage of darkly pigmented rib tips (a), and a bar plot depicting the proportion of shells classified as either lightly colored (no fill) or dark (black fill) by island. It should be noted that KA represents two sites and the site with lightly colored CaCO3 substratum had a higher proportion of light shells than the other site with dark basalt substratum. All other sites had dark basalt substratum.

Figure 4. Scatterplots of (a) surface area, (b) height index, and (c) doming index versus latitude. Points are the median observed values and error bars represent 68% (thick) and 95% (thin) credible intervals. Regression lines represent the best-fit model of the medians with dark grey ribbons showing the 68% credible interval and the light grey ribbons representing the 95% credible intervals. The letters in each panel represent statistical groupings based on pairwise Tukey tests among site coefficients as determined by the model. Sites with differing grouping letters had significant differences in the means. If sites within the same island have one letter, they were in the same grouping.

Figure 5. Scatter plots of the variances in (a) surface area, (b) height index, and (c) doming index versus location. Points are the median observed values and error bars represent 68% (thick) and 95% (thin) credible intervals. Regression lines represent the best-fit model of the medians with dark grey ribbons showing the 68% credible interval and the light grey ribbons representing the 95% credible intervals. The letters in each panel represent statistical groupings based on pairwise Tukey tests among site coefficients as determined by the model. Sites with differing grouping letters had significant differences in the means. If sites within the same island have one letter, they were in the same grouping.

Figure 6. Scatter plot of shell height index versus width index for all shells. Triangles on y-axis represent lateral shell profile dimensions and the ellipse and circle on the x-axis represent the aperture dimensions. Heat dissipation through the shell is maximized at a width index of 1 and a larger height index. Predation avoidance due to apex crushing and laterally applied forces is maximized at a width index of 1 and a smaller height index. Note that the range of both axes is 0.5 to accurately depict the broader distribution of heights than widths.

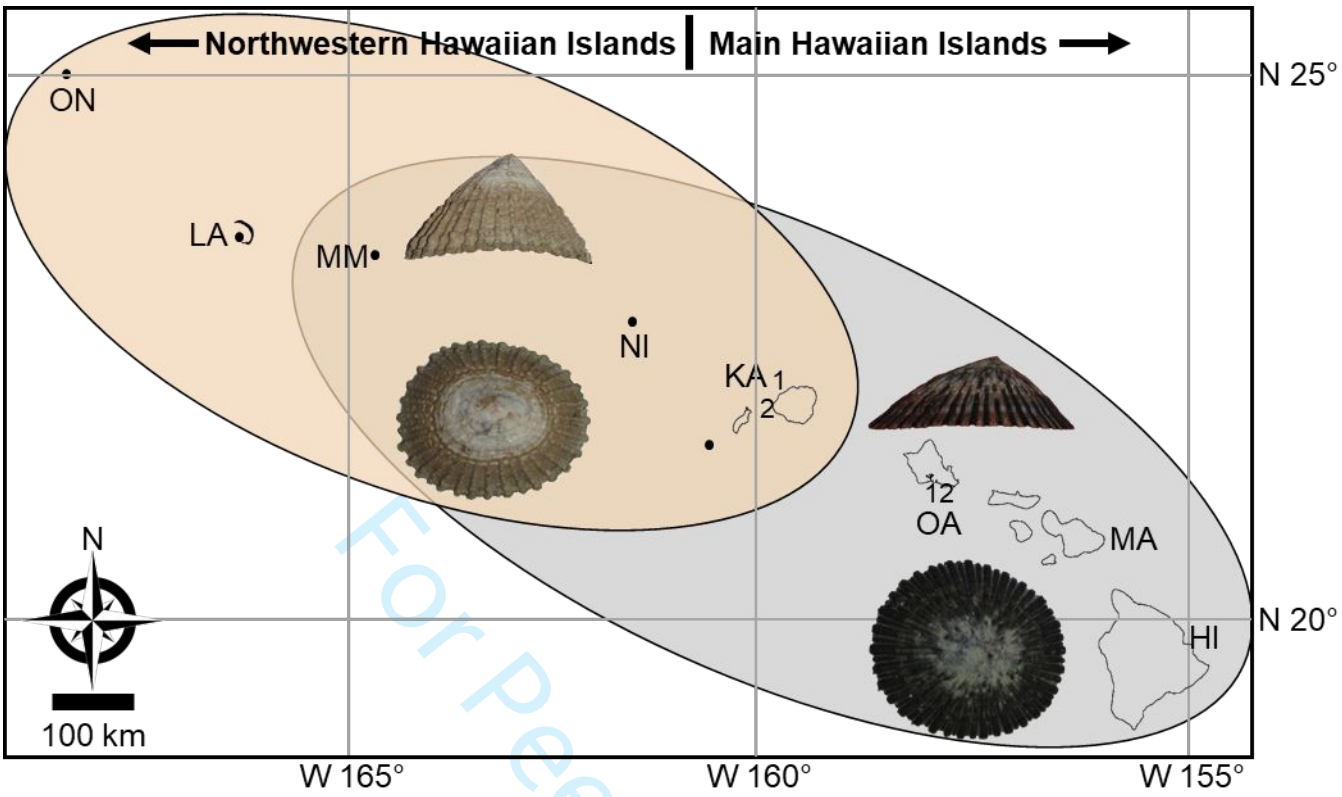

Figure 1. Map of Hawaiian Archipelago. Sampling sites are labeled by either the island abbreviation or, when there were multiple sites, the site number (as described in Table 1). The biogeographic range of color morphotypes observed in the samples is represented by the filled ovals (peach – lighter shells, grey – darker shells. A photograph of an example shell of each color morphotype from a ventral and dorsal perspective is shown near the islands typically harboring those morphs.

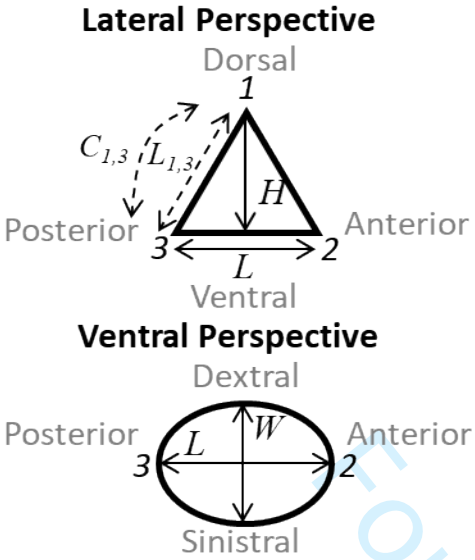

Figure 2. Diagram of shell measurements and landmarks from lateral and ventral perspectives. The numbers represent Cartesian coordinates obtained from photographs, and the letters represent characters: *L* = length, *W* = width, *C* = distance following the edge of the shell which was generally curvilinear. Solid lines represent measurements made with calipers, and dashed lines represent measurements made using photographs.

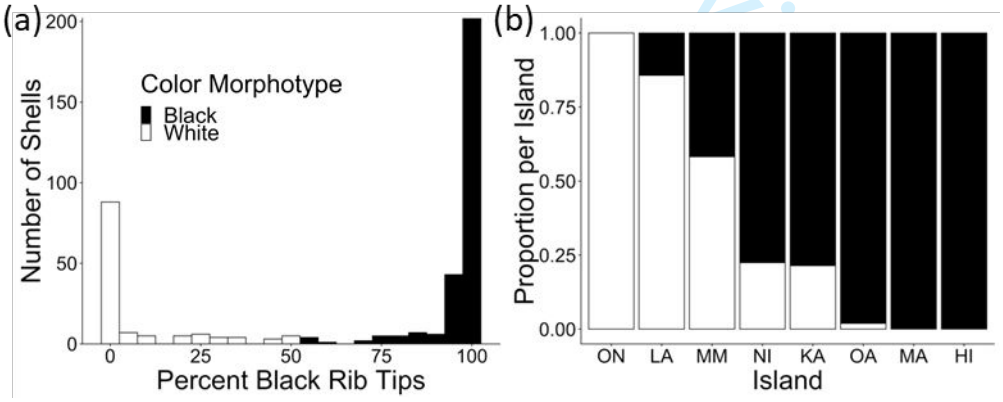

Figure 3. Histogram of the number of shells that had a given percentage of darkly pigmented rib tips (a), and a bar plot depicting the proportion of shells classified as either lightly colored (no fill) or dark (black fill) by island. It should be noted that KA represents two sites and the site with lightly colored CaCO3 substratum (KA2) had a higher proportion of light shells than the other site with dark basalt substratum (KA1). All other sites had dark basalt substratum (Table 1).

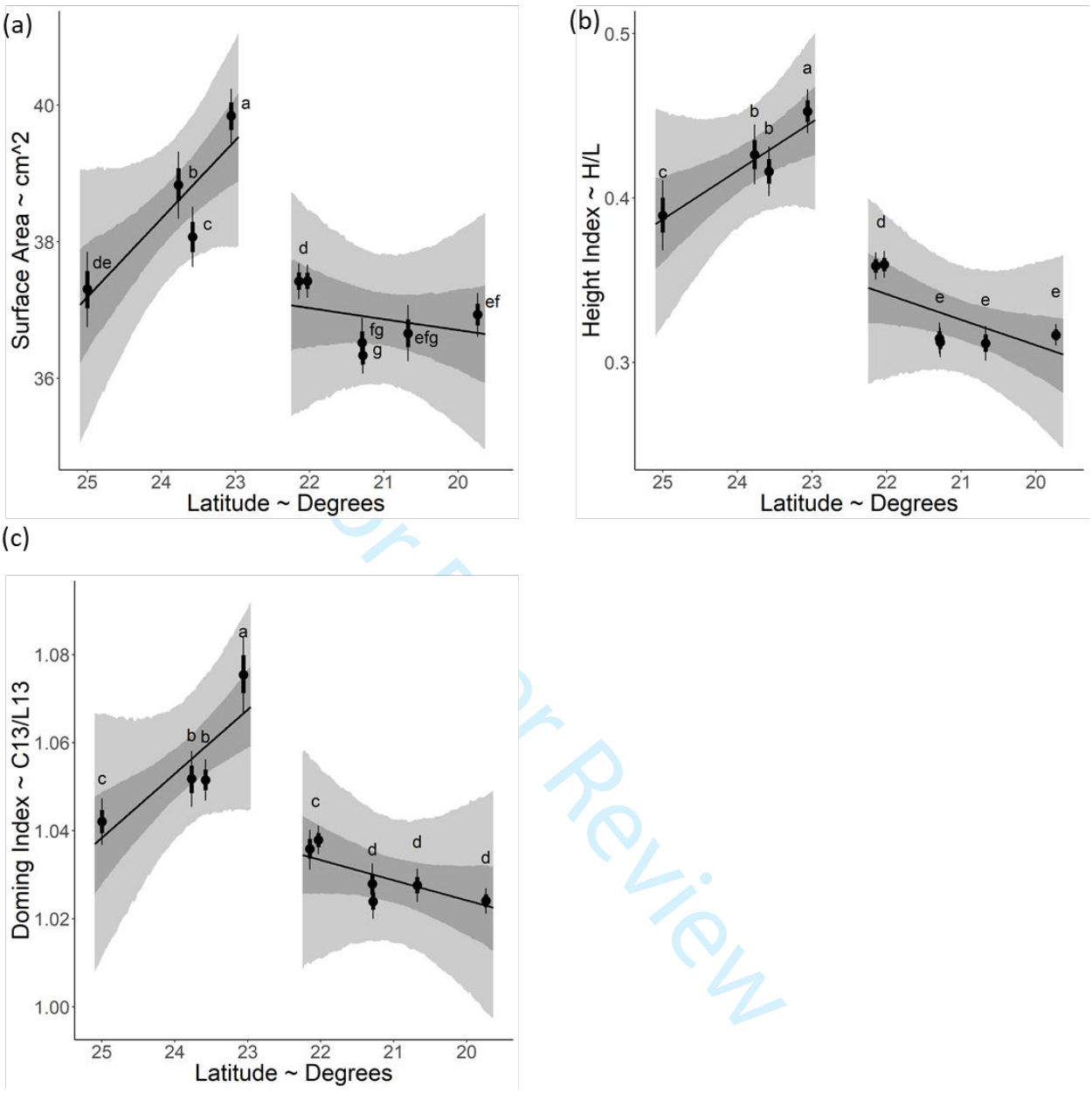

Figure 4. Scatterplots of (a) surface area, (b) height index, and (c) doming index versus latitude. Points are the median observed values and error bars represent 68% (thick) and 95% (thin) credible intervals. Regression lines represent the best-fit model of the medians with dark grey ribbons showing the 68% credible interval and the light grey ribbons representing the 95% credible intervals. The letters in each panel represent statistical groupings based on pairwise Tukey tests among site coefficients as determined by the model. Sites with differing grouping letters had significant differences in the means. If sites within the same island have one letter, they were in the same grouping.

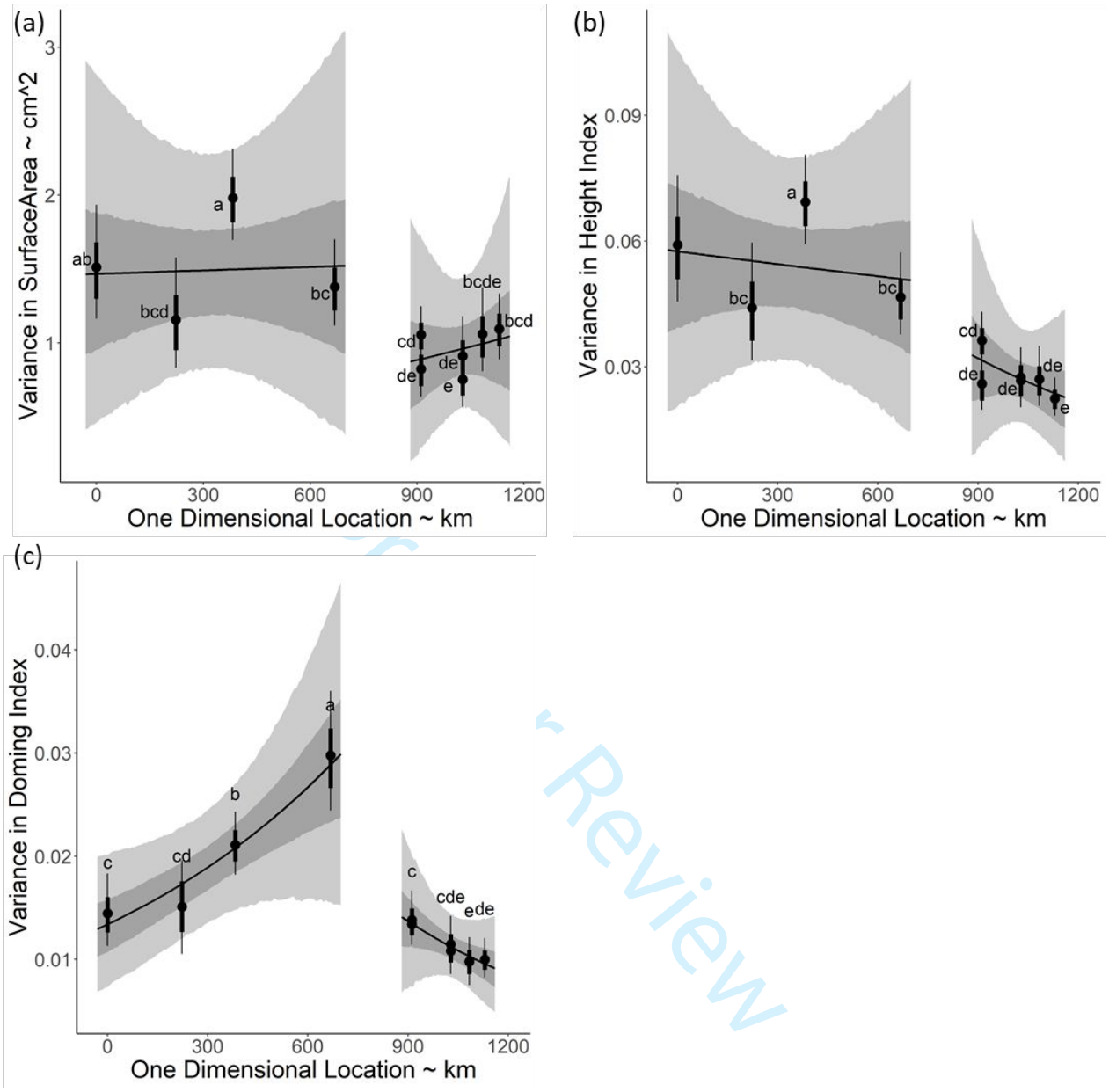

Figure 5. Scatter plots of the variances in (a) surface area, (b) height index, and (c) doming index versus location. Points are the median observed values and error bars represent 68% (thick) and 95% (thin) credible intervals. Regression lines represent the best-fit model of the medians with dark grey ribbons showing the 68% credible interval and the light grey ribbons representing the 95% credible intervals. The letters in each panel represent statistical groupings based on pairwise Tukey tests among site coefficients as determined by the model. Sites with differing grouping letters had significant differences in the means. If sites within the same island have one letter, they were in the same grouping.

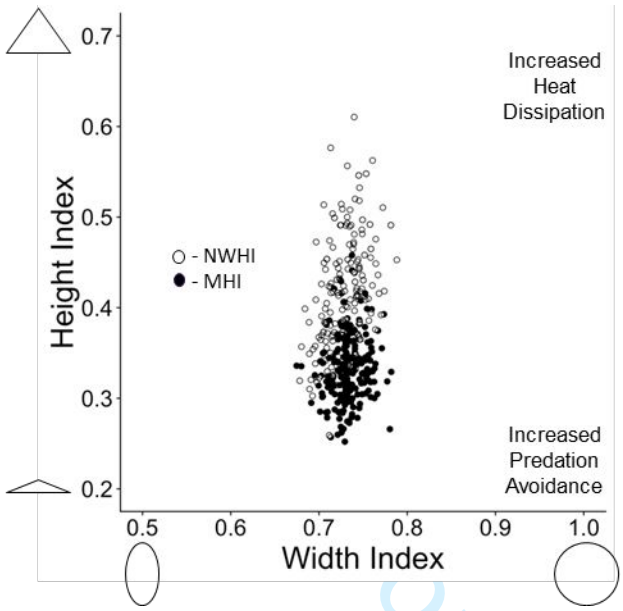

Figure 6. Scatter plot of shell height index versus width index for all shells. Triangles on y-axis represent lateral shell profile dimensions and the ellipse and circle on the x-axis represent the aperture dimensions. Heat dissipation through the shell is maximized at a width index of 1 and a larger height index. Predation avoidance due to apex crushing and laterally applied forces is maximized at a width index of 1 and a smaller height index. Note that the range of both axes is 0.5 to accurately depict the broader distribution of heights than widths.

DATA AVAILABILTY

The data and scripts used in this manuscript are available at https://github.com/jdselwyn/Opihi_Morphology and www.dryad.org.

REFERENCES

Agrawal, A. A., Conner, J. K., & Rasmann, S. (2010). Tradeoffs and Negative Correlations In Evolutionary Ecology. *Evolution After Darwin: The First 150 Years*, 243-268.

Athens, J. S., Rieth, T. M., & Dye, T. S. (2014). A Paleoenvironmental and Archaeological Model-Based Age Estimate for the Colonization of Hawai'i. *American Antiquity*, *79*(1), 144-155.

Bekkevold, D., André, C., Dahlgren, T. G., Clausen, L. A. W., Torstensen, E., Mosegaard, H., … Ruzzante, D. E. (2005). Environmental Correlates of Population Differentiation in Atlantic Herring. *Evolution*, *59*(12), 2656–2668.

Belonsky, G. M., & Kennedy, B. W. (1988). Selection on Individual Phenotype and Best Linear Unbiased Predictor of Breeding Value in a Closed Swine Herd. *Journal of Animal Science*, *66*(5), 1124–1131.

Bent, A. C. (1929). *Life Histories of North American Shore Birds: In Two Parts*. Dover Publications, Incorporated.

Beukers, J. S., & Jones, G. P. (1998). Habitat complexity modifies the impact of piscivores on a coral reef fish population. *Oecologia*, *114*(1), 50–59.

Bird, C. E., Franklin, E. C., Smith, C. M., & Toonen, R. J. (2013). Between tide and wave marks: a unifying model of physical zonation on littoral shores. *PeerJ*, *1*, e154.

Bird, C. E., Holland, B. S., Bowen, B. W., & Toonen, R. J. (2007). Contrasting phylogeography in three endemic Hawaiian limpets (Cellana spp.) with similar life histories. *Molecular Ecology*, *16*(15), 3173–3186.

Bird, C. E., Holland, B. S., Bowen, B. W., & Toonen, R. J. (2011). Diversification of sympatric broadcast-spawning limpets (Cellana spp.) within the Hawaiian archipelago. *Molecular Ecology*, *20*(10), 2128–2141.

Blondel, J. (2008). On humans and wildlife in Mediterranean islands. *Journal of Biogeography*, *35*(3), 509–518.

Bowen, B. W., Rocha, L. A., Toonen, R. J., & Karl, S. A. (2013). The origins of tropical marine biodiversity. *Trends in Ecology & Evolution*, *28*(6), 359-366.

Branch, G. M., Trueman, E. R., & Clarke, M. R. (1985). Limpets: evolution and adaptation. *The Mollusca*, 187-220.

Bryant, E. H., & Meffert, L. M. (1993). The effect of serial founder-flush cycles on quantitative genetic variation in the housefly. *Heredity*, *70*(2), 122.

Bürkner, P. (2017). brms: An R Package for Bayesian Multilevel Models Using Stan. *Journal of Statistical Software, 80*(1), 1 - 28.

Cinner, J. E., Graham, N. A., Huchery, C., & MacNeil, M. A. (2013). Global effects of local human population density and distance to markets on the condition of coral reef fisheries. *Conservation Biology*, *27*(3), 453-458.

Cockett, P. M. (2015). *Population Composition of an Exploited Hawaiian Fishery* (Master's Thesis, Texas A&M University - Corpus Christi).

Dann, P. (2005). Is bill length in curlews Numenius associated with foraging habitats and diet in non-breeding grounds. *Wader Study Group Bulletin*, *106*, 60-61.

DeFaveri, J., Jonsson, P. R., & Merilä, J. (2013). Heterogeneous Genomic Differentiation in Marine Threespine Sticklebacks: Adaptation Along an Environmental Gradient. *Evolution*, *67*(9), 2530–2546.

Denny, M. W. (2000). Limits to optimization: fluid dynamics, adhesive strength and the evolution of shape in limpet shells. *Journal of Experimental Biology*, *203*(17), 2603–2622.

Denny, M. W., Dowd, W. W., Bilir, L., & Mach, K. J. (2011). Spreading the risk: Small-scale body temperature variation among intertidal organisms and its implications for species persistence. *Journal of Experimental Marine Biology and Ecology*, *400*(1), 175–190.

Denny, M. W., & Harley, C. D. G. (2006). Hot limpets: predicting body temperature in a conductance-mediated thermal system. *Journal of Experimental Biology*, *209*(13), 2409–2419.

Dillon, M. E., Liu, R., Wang, G., & Huey, R. B. (2012). Disentangling thermal preference and the thermal dependence of movement in ectotherms. *Journal of Thermal Biology*, *37*(8), 631-639.

Duputié, A., Massol, F., Chuine, I., Kirkpatrick, M., & Ronce, O. (2012). How do genetic correlations affect species range shifts in a changing environment? *Ecology Letters*, *15*(3), 251–259.

Emory, K. P. (1928). *Archaeology of Nihoa and Necker islands* (Vol. 9). Honolulu, HI: Bishop Museum Press.

Friedlander, A. M., & DeMartini, E. E. (2002). Contrasts in density, size, and biomass of reef fishes between the northwestern and the main Hawaiian islands: the effects of fishing down apex predators. *Marine Ecology Progress Series*, *230*, 253–264.

Futuyma, D. J. (2013). *Evolution. Third Edition.* Sunderland, Massachusetts U.S.A: Sinauer Associates, Inc. Publishers.

Gauthier, P., Lumaret, R., & Bédécarrats, A. (1998). Ecotype differentiation and coexistence of two parapatric tetraploid subspecies of cocksfoot (Dactylis glomerata) in the Alps. *The New Phytologist*, *139*(4), 741–750.

Geen, M. R. S., & Johnston, G. R. (2014). Coloration affects heating and cooling in three color morphs of the Australian bluetongue lizard, Tiliqua scincoides. *Journal of Thermal Biology*, *43*, 54–60.

Gelman, A., Lee, D., & Guo, J. (2015). Stan: A probabilistic programming language for Bayesian inference and optimization. *Journal of Educational and Behavioral Statistics*, *40*(5), 530-543.

Gunderson, A. R., & Stillman, J. H. (2015). Plasticity in thermal tolerance has limited potential to buffer ectotherms from global warming. *Proceedings of the Royal Society B: Biological Sciences*, *282*(1808), 20150401.

Guo, B., DeFaveri, J., Sotelo, G., Nair, A., & Merilä, J. (2015). Population genomic evidence for adaptive differentiation in Baltic Sea three-spined sticklebacks. *BMC Biology*, *13*(1), 19.

Harley, C. D. G., Denny, M. W., Mach, K. J., & Miller, L. P. (2009). Thermal stress and morphological adaptations in limpets. *Functional Ecology*, *23*(2), 292–301.

Hays, W. S. T., & Conant, S. (2007). Biology and Impacts of Pacific Island Invasive Species. 1. A Worldwide Review of Effects of the Small Indian Mongoose, Herpestes javanicus (Carnivora: Herpestidae). *Pacific Science*, *61*(1), 3–16.

Hoekstra, H. E., Hoekstra, J. M., Berrigan, D., Vignieri, S. N., Hoang, A., Hill, C. E., … Kingsolver, J. G. (2001). Strength and tempo of directional selection in the wild. *Proceedings of the National Academy of Sciences*, *98*(16), 9157–9160.

Heino, M., Pauli, B. D., & Dieckmann, U. (2015). Fisheries-induced evolution. Annual Review Of Ecology, Evolution, and Systematics, 46.

Hendry, A. P., Gotanda, K. M., & Svensson, E. I. (2017). Human influences on evolution, and the ecological and societal consequences. *Philosophical Transactions of the Royal Society B: Biological Sciences,* 372, 20160028.

Hines, H. N., Morriss, H., Saunders, K., Williams, R. L., Young, S. L., & Stafford, R. (2017). Localized versus regional adaptation in limpet shell morphology across the Iberian Peninsula. *Marine Ecology*, 38(6), e12472.

James, H. F., & Burney, D. A. (1997). The diet and ecology of Hawaii's extinct flightless waterfowl: evidence from coprolites. *Biological Journal of the Linnean Society*, *62*(2), 279–297.

Johnson, T., & Barton, N. (2005). Theoretical models of selection and mutation on quantitative traits. *Philosophical Transactions of the Royal Society B: Biological Sciences*, 360(1459), 1411-1425.

Julian Caley, M., & Schluter, D. (2003). Predators favour mimicry in a tropical reef fish. *Proceedings of the Royal Society of London. Series B: Biological Sciences*, *270*(1516), 667–672.

Kay, E. A., & Magruder, W. (1977). The biology of opihi. *Department of Planning and Economic Development, Honolulu*, 46.

Kass, R. E., & Raftery, A. E. (1995). Bayes Factors. *Journal of the American Statistical Association*, *90*(430), 773–795.

Kemp, P., & Bertness, M. D. (1984). Snail shape and growth rates: Evidence for plastic shell allometry in Littorina littorea. *Proceedings of the National Academy of Sciences*, *81*(3), 811–813.

Kikiloi, K., Friedlander, A. M., Wilhelm, A., Lewis, N. A., Quiocho, K., 'Āila Jr, W., & Kaho'ohalahala, S. (2017). Papahānaumokuākea: integrating culture in the design and management of one of the world's largest marine protected areas. *Coastal Management*, 45(6), 436-451.

Knight, K. (2011). Intertidal Snails Are Thermally Insensitive. *Journal of Experimental Biology*, *214*(21), iii–iii.

Kuparinen, A., & Festa-Bianchet, M. (2017). Harvest-induced evolution: insights from aquatic and terrestrial systems. *Philosophical Transactions of the Royal Society B: Biological Sciences*, 372(1712), 20160036.

Lande, R., & Arnold, S. J. (1983). The Measurement of Selection on Correlated Characters. *Evolution*, *37*(6), 1210–1226.

Lathlean, J. A., McWilliam, R. A., Ayre, D. J., & Minchinton, T. E. (2015). Biogeographical patterns of rocky shore community structure in south-east Australia: effects of oceanographic conditions and heat stress. *Journal of Biogeography*, *42*(8), 1538–1552.

Lemos, B., Meiklejohn, C. D., Cáceres, M., & Hartl, D. L. (2005). Rates of Divergence in Gene Expression Profiles of Primates, Mice, and Flies: Stabilizing Selection and Variability Among Functional Categories. *Evolution*, *59*(1), 126–137.

Leonard, G. H., Bertness, M. D., & Yund, P. O. (1999). Crab Predation, Waterborne Cues, and Inducible Defenses in the Blue Mussel, Mytilus Edulis. *Ecology*, *80*(1), 1–14.

Lind, M. I., Ingvarsson, P. K., Johansson, H., Hall, D., & Johansson, F. (2011). Gene Flow And Selection On Phenotypic Plasticity In An Island System Of Rana Temporaria: Gene Flow And Selection On Phenotypic Plasticity. *Evolution*, *65*(3), 684–697.

Link, W. A., & Barker, R. J. (2006). Model Weights and the Foundations of Multimodel Inference. *Ecology*, *87*(10), 2626–2635.

Lleonart, J., Salat, J., & Torres, G. J. (2000). Removing allometric effects of body size in morphological analysis. *Journal of Theoretical Biology*, 205(1), 85-93.

Lowell, R. B. (1984). Desiccation of intertidal limpets: Effects of shell size, fit to substratum, and shape. *Journal of Experimental Marine Biology and Ecology*, *77*(3), 197–207.

Lowell, R. B. (1986). Crab predation on limpets: predator behavior and defensive features of the shell morphology of the prey. *The Biological Bulletin*, *171*(3), 577–596.

Manríquez, P. H., Lagos, N. A., Jara, M. E., & Castilla, J. C. (2009). Adaptive shell color plasticity during the early ontogeny of an intertidal keystone snail. *Proceedings of the National Academy of Sciences*, *106*(38), 16298–16303.

Marshall, W. (1980). *Feeding behaviour and ecology of the turnstone (Arenaria interpres) on a rocky shore and in captivity*. Retrieved from https://www.era.lib.ed.ac.uk/handle/1842/12575

Matisoo-Smith, E., Roberts, R. M., Irwin, G. J., Allen, J. S., Penny, D., & Lambert, D. M. (1998). Patterns of prehistoric human mobility in Polynesia indicated by mtDNA from the Pacific rat. *Proceedings of the National Academy of Sciences*, *95*(25), 15145–15150.

McCoy, M. D. (2008). Hawaiian Limpet Harvesting in Historical Perspective: A Review of Modern and Archaeological Data on Cellana spp. from the Kalaupapa Peninsula, Moloka ʻi Island. *Pacific Science*, 62(1), 21-39.

McCoy, P. C., & Nees, R. (2013). Archaeological Inventory Survey of the Mauna Kea Ice Age Natural Area Reserve, Ka ʻohe Ahupua ʻa, Hāmākua District, Island of Hawaiʻi. *Prepared for the Division of Forestry and Wildlife, Natural Reserves System, Honolulu*

Mercurio, K. S., Palmer, A. R., & Lowell, R. B. (1985). Predator-mediated microhabitat partitioning by two species of visually cryptic, intertidal limpets. *Ecology*, 66(5), 1417-1425.

Meiri, S. (2008). Evolution and ecology of lizard body sizes. *Global Ecology and Biogeography*, *17*(6), 724–734.

Merilaita, S., Lyytinen, A., & Mappes, J. (2001). Selection for cryptic coloration in a visually heterogeneous habitat. *Proceedings of the Royal Society of London. Series B: Biological Sciences*, *268*(1479), 1925–1929.

Merilaita, S., Scott-Samuel, N. E., & Cuthill, I. C. (2017). How camouflage works. *Philosophical Transactions of the Royal Society B: Biological Sciences*, 372(1724), 20160341.

Miller, L. P., & Denny, M. W. (2011). Importance of Behavior and Morphological Traits for Controlling Body Temperature in Littorinid Snails. *The Biological Bulletin*, *220*(3), 209–223.

Kay, E. A. & Schoenberg-Dole (1991). Shells of Hawai'i. Honolulu, HI: University of Hawai'i Press.

Olson, S. L., & James, H. F. (1982). Fossil Birds from the Hawaiian Islands: Evidence for Wholesale Extinction by Man Before Western Contact. *Science*, *217*(4560), 633–635.

Pavlova, A., Amos, J. N., Joseph, L., Loynes, K., Austin, J. J., Keogh, J. S., … Sunnucks, P. (2013). Perched at the Mito-Nuclear Crossroads: Divergent Mitochondrial Lineages Correlate with Environment in the Face of Ongoing Nuclear Gene Flow in an Australian Bird. *Evolution*, *67*(12), 3412–3428.

Payne, N. L., & Smith, J. A. (2017). An alternative explanation for global trends in thermal tolerance. *Ecology Letters*, 20(1), 70-77.

Pennell, S., & Deignan, J. (1989). Computing the Projected Area of a Cone. *SIAM Review*, *31*(2), 299–302.

Pereboom, J. J. M., & Biesmeijer, J. C. (2003). Thermal constraints for stingless bee foragers: the importance of body size and coloration. *Oecologia*, *137*(1), 42–50.

Pinsky, M. L., Eikeset, A. M., McCauley, D. J., Payne, J. L., & Sunday, J. M. (2019). Greater vulnerability to warming of marine versus terrestrial ectotherms. *Nature*, *569*(7754), 108–111.

Pintor, A. F., Schwarzkopf, L., & Krockenberger, A. K. (2016). Extensive acclimation in ectotherms conceals interspecific variation in thermal tolerance limits. *Plos One*, 11(3), e0150408.

R Core Team (2018). *R: A language and environment for statistical computing*. R Foundation for Statistical Computing, Vienna, Austria.

Rainey, P. B., & Travisano, M. (1998). Adaptive radiation in a heterogeneous environment. *Nature*, *394*(6688), 69.

Ratner, S., & Lande, R. (2001). Demographic and Evolutionary Responses to Selective Harvesting in Populations with Discrete Generations. *Ecology*, *82*(11), 3093–3104.

Reeb, C. (1995). *Molecular Insights into the Evolution of a Circumtropical Fish (Coryphaena hippurus) and an Indo-Pacific Group of Mollusks (Cellana)* (Doctoral Dissertation, University of Hawai'i at Mānoa).

Rogers, A. J., & Weisler, M. I. (2019). Assessing the Efficacy of Genus-Level Data in Archaeomalacology: A Case Study of the Hawaiian Limpet (Cellana spp.), Moloka ʻi, Hawaiian Islands. *The Journal of Island and Coastal Archaeology*, 1-29.

Schemske, D. W. (1984). Population Structure and Local Selection in Impatiens Pallida (balsaminaceae), a Selfing Annual. *Evolution*, *38*(4), 817–832.

Schneider, C. A., Rasband, W. S., & Eliceiri, K. W. (2012). NIH Image to ImageJ: 25 years of image analysis. *Nature Methods*, *9*(7), 671–675.

Seabra, R., Wethey, D. S., Santos, A. M., & Lima, F. P. (2011). Side matters: Microhabitat influence on intertidal heat stress over a large geographical scale. *Journal of Experimental Marine Biology and Ecology*, *400*(1), 200–208.

Serruys, M., & Van Dyck, H. (2014). Development, survival, and phenotypic plasticity in anthropogenic landscapes: trade-offs between offspring quantity and quality in the nettle-feeding peacock butterfly. *Oecologia*, *176*(2), 379–387.

Seuront, L., & Ng, T. P. (2016). Standing in the sun: infrared thermography reveals distinct thermal regulatory behaviours in two tropical high-shore littorinid snails. *Journal of Molluscan Studies*, 82(2), 336-340.

Shepard, D. B., & Burbrink, F. T. (2011). Local-scale environmental variation generates highly divergent lineages associated with stream drainages in a terrestrial salamander, Plethodon caddoensis. *Molecular Phylogenetics and Evolution*, *59*(2), 399–411.

Snyder, C. W. (2016). Evolution of global temperature over the past two million years. *Nature*, 538(7624), 226.

Somero, G. N. (2002). Thermal physiology and vertical zonation of intertidal animals: optima, limits, and costs of living. *Integrative and comparative biology*, *42*(4), 780-789.

Sorensen, F. E., & Lindberg, D. R. (1991). Preferential predation by American black oystercatchers on transitional ecophenotypes of the limpet Lottia pelta (Rathke). *Journal of Experimental Marine Biology and Ecology*, 154(1), 123-136.

Teske, P. R., Barker, N. P., & McQuaid, C. D. (2007). Lack of genetic differentiation among four sympatric southeast African intertidal limpets (Siphonariidae): phenotypic plasticity in a single species? *Journal of Molluscan Studies*, *73*(3), 223–228.

Tom, S. K. (2011). *An investigation of the cultural use and population characteristics of ʼopihi (Mollusca: Cellana spp.) at Kalaupapa National Historical Park* (Master's Thesis, University of Hawaiʻi at Hilo).

Toonen, R. J., Andrews, K. R., Baums, I. B., Bird, C. E., Concepcion, G. T., Daly-Engel, T. S., … Bowen, B. W. (2011). Defining Boundaries for Ecosystem-Based Management: A Multispecies Case Study of Marine Connectivity across the Hawaiian Archipelago. *Journal of Marine Biology, 2011.*

Trullas, S. C., van Wyk, J. H., & Spotila, J. R. (2007). Thermal melanism in ectotherms. *Journal of Thermal Biology*, 32(5), 235-245.

Trussell, G. C. (1996). Phenotypic Plasticity in an Intertidal Snail: The Role of a Common Crab Predator. *Evolution*, *50*(1), 448–454.

Trussell, G. C. (2000). Phenotypic Clines, Plasticity, and Morphological Trade-Offs in an Intertidal Snail. *Evolution*, *54*(1), 151–166.

Vehtari, A., Gelman, A., & Gabry, J. (2017). Practical Bayesian model evaluation using leave-one-out cross-validation and WAIC. *Statistics and Computing*, *27*(5), 1413–1432.

Vehtari, A., Gelman, A., Simpson, D., Carpenter, B., & Bürkner, P. C. (2019). Rank-normalization, folding, and localization: An improved Rˆ for assessing convergence of MCMC. arXiv preprint arXiv:1903.08008.

Verheyen, J., & Stoks, R. (2019). Temperature variation makes an ectotherm more sensitive to global warming unless thermal evolution occurs. *Journal of Animal Ecology, 88*(4), 624-636.

Vermeij, G. J. (1973). Morphological patterns in high-intertidal gastropods: Adaptive strategies and their limitations. *Marine Biology*, *20*(4), 319–346.

Wadgymar, S. M., Lowry, D. B., Gould, B. A., Byron, C. N., Mactavish, R. M., & Anderson, J. T. (2018). Identifying targets and agents of selection: innovative methods to evaluate the processes that contribute to local adaptation. *Methods in Ecology and Evolution*, 738–749.

Whiteman, C. D. (2000). *Mountain meteorology: fundamentals and applications*. Oxford University Press.

Whitfield, D. P. (1985). *Social organisation and feeding behaviour of wintering turnstone (Arenaria interpres)* (Doctoral Dissertation). Retrieved from Edinburgh Research Archive. (Accession 1842/14660)

Wickham, H. (2017). tidyverse: Easily Install and Load the 'Tidyverse'. R package version 1.2.1. https://CRAN.R-project.org/package=tidyverse

Williams, I. D., Walsh, W. J., Schroeder, R. E., Friedlander, A. M., Richards, B. L., & Stamoulis, K. A. (2008). Assessing the importance of fishing impacts on Hawaiian coral reef fish assemblages along regional-scale human population gradients. *Environmental Conservation*, 35(3), 261-272.

Wren, J. L., Kobayashi, D. R., Jia, Y. and Toonen, R. J., 2016. Modeled population connectivity across the Hawaiian archipelago. *Plos One*, 11(12), p.e0167626.

BIOSKETCHES

Ashley M. Hamilton is an undergraduate student who is broadly interested in evolutionary biology and the mechanisms of selection. Her work focuses on the phenotypic and genetic

patterns associated with evolutionary change in a variety of systems, with a special focus on plant systems.

Jason D. Selwyn is interested in the causes and consequences of variations in dispersal dynamics. His research focuses on understanding the environmental factors leading to dispersal variation in Caribbean reef gobies.

Rebecca M. Hamner has broad interests in conservation biology, molecular ecology, and evolution. Her current work focuses on applying genomic tools to answer questions related to the conservation and management of threatened and culturally important species.

Hoku Johnson is interested in human uses of the nearshore environment and indigenous connections to place, focusing on Native Hawaiian gathering practices, local stewardship of marine resources, and ways state and federal regulations influence community health.

Tia Brown is interested in Hawaii's marine ecosystems, particularly nearshore and intertidal ecosystems science. Her focus centers on ways to weave traditional Hawaiian knowledge and practices together with modern-day science and technology to maintain the health, beauty, and wealth of Hawaii's natural resources and serve as a model for the rest of the world.

Shauna Kēhaunani Springer is interested intertidal and nearshore ecosystems. She focuses on understanding and incorporating traditional Hawaiian monitoring and customary practices into her research and building community capacity around these efforts.

Christopher E. Bird is an Associate Professor that uses molecular and computational tools to study the evolution of marine life on ecological time scales to facilitate marine resource management and conservation.

Author contributions: Project conception: CEB. Sample collection: HKJ, TB, KS, CEB; Character state scoring: AMH, RMH, HKJ, TB, KS, CEB; Data processing and analysis: AMH, RMH, JDS, CEB; Writing and editing: all authors.

SUPPLEMENTARY TABLES & FIGURES

Table S1. Imputation of missing length and width results. *RSE* is the residual standard error. See Figure 2 for the definition of the measurements.

Imputation Variable	AIC Linear Model	AIC Power Model	Equation of Best Model	RSE (mm)
L	1599	1472	$L = 1.645\ W^{0.9180}$	0.402
W	1459	1322	$W = 0.6038\ L^{1.079}$	0.309

Table S2. Results from allometric normalization of morphometric characters to the mean shell length. See Figure 2 for the definition of the measurements. The degrees of freedom of the tests are indicated in the subscripts of χ^2.

Measurement for Normalization	Equation of best fit model	Log Likelihood Ratio	*p*	Residual Standard Error (mm)	Variance Structure Modeled
W	$W = 0.6089\ L^{1.076}$	$\chi^2_{2,4} = 2790$	<0.0001	0.283	Y
H	$\ln(H) = 0.1933\ \ln(L)^{2.055}$	$\chi^2_{2,3} = 1171$	<0.0001	1.197	N
$C_{1,3}$	$\ln(C_{1,3}) = 0.7585\ \ln(L)^{1.151}$	$\chi^2_{2,4} = 1912$	<0.0001	1.032	Y
$L_{1,3}$	$\ln(L_{1,3}) = 0.7479\ \ln(L)^{1.152}$	$\chi^2_{2,4} = 2173$	<0.0001	1.021	Y

Table S3. Results of *a priori* hypothesis tests for the relationships between the morphometric characters associated with thermal avoidance and human inhabitance. CI.Lower and CI.Upper are the 95% bounds of the confidence interval. The Evid.Ratio is the Bayes Factor. The Post.Prob is the posterior probability. Inf is infinite.

Parameter	Hypothesis	Translation	Estimate	Est.Error	CI.Lower	CI.Upper	Evid.Ratio	Post.Prob
Surface Area	b_latitude.c + b_latitude.c:island_groupNWHI = 0	NWHI mean is zero	-1.15	0.69	-2.52	0.24	NA	NA
	b_latitude.c = 0	MHI mean is zero	0.16	0.53	-0.93	1.22	NA	NA
	b_latitude.c + b_latitude.c:island_groupNWHI < b_latitude.c	compare slopes NWHI vs MHI	-1.31	0.87	-Inf	0.06	17.15	0.94
	b_Intercept + b_island_groupNWHI > b_Intercept	compare means NWHI vs MHI	3.28	1.45	1.03	Inf	56.49	0.98
Doming	b_latitude.c + b_latitude.c:island_groupNWHI = 0	NWHI mean is zero	-0.01	0.01	-0.04	0.01	NA	NA
	b_latitude.c = 0	MHI mean is zero	0	0.01	-0.01	0.02	NA	NA

	b_latitude.c + b_latitude.c:island_groupNWHI < b_latitude.c	compare slopes NWHI vs MHI	-0.02	0.01	-Inf	0	17.59	0.95
	b_Intercept + b_island_groupNWHI > b_Intercept	compare means NWHI vs MHI	0.04	0.02	0.01	Inf	45.69	0.98
Height								
	b_latitude.c + b_latitude.c:island_groupNWHI = 0	NWHI mean is zero	-0.03	0.02	-0.08	0.02	NA	NA
	b_latitude.c = 0	MHI mean is zero	0.01	0.02	-0.02	0.05	NA	NA
	b_latitude.c + b_latitude.c:island_groupNWHI < b_latitude.c	compare slopes NWHI vs MHI	-0.04	0.03	-Inf	0	16.88	0.94
	b_Intercept + b_island_groupNWHI > b_Intercept	compare means NWHI vs MHI	0.12	0.05	0.05	Inf	71.67	0.99
Variability in Surface Area	b_sigma_island_groupNWHI:Location.c = 0"	NWHI mean is zero	0	0	0	0	NA	NA
	b_sigma_island_groupMHI:Location.c = 0	MHI mean is zero	0	0	0	0.01	NA	NA

	b_sigma_island_groupNWHI:Location.c > b_sigma_island_groupMHI:Location.c	compare slopes NWHI vs MHI	0	0	-Inf	0	1.57	0.61
	b_sigma_island_groupNWHI > b_sigma_Intercept	compare means NWHI vs MHI	0.61	0.91	-0.74	Inf	4.49	0.82
Variability in Doming	b_latitude.c + b_latitude.c:island_groupNWHI = 0	NWHI mean is zero	0	0	0	0	NA	NA
	b_latitude.c = 0	MHI mean is zero	0	0	0	0	NA	NA
	b_latitude.c + b_latitude.c:island_groupNWHI < b_latitude.c	compare slopes NWHI vs MHI	0	0	0	Inf	21.49	0.96
	b_Intercept + b_island_groupNWHI > b_Intercept	compare means NWHI vs MHI	4.3	0.54	3.51	Inf	4165.67	1
Variability in Height	b_latitude.c + b_latitude.c:island_groupNWHI = 0	NWHI mean is zero	0	0	0	0	NA	NA
	b_latitude.c = 0	MHI mean is zero	0	0	0	-0.01	NA	NA

b_latitude.c + b_latitude.c:island_groupNWHI < b_latitude.c	compare slopes NWHI vs MHI	0	0	-Inf	0.01	0.39	0.28
b_Intercept + b_island_groupNWHI > b_Intercept	compare means NWHI vs MHI	4.05	0.83	2.82	Inf	728.93	1

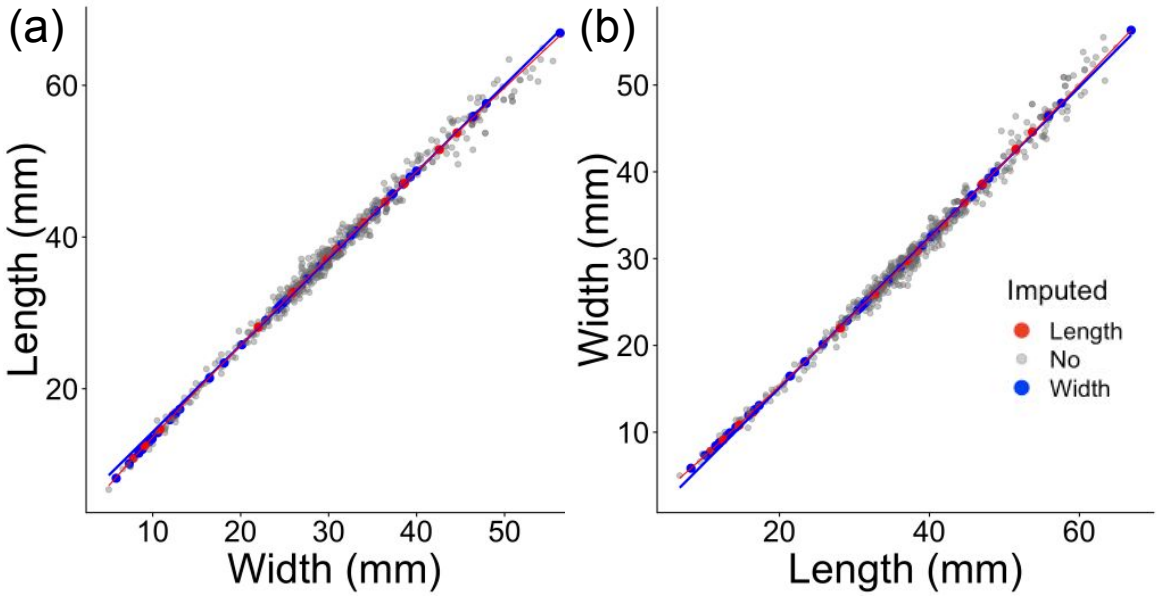

Figure S1. Scatterplot of (a) shell length versus width and (b) shell width versus length. The equations of the best-fit lines (Table S1) were used to impute missing measurements due to damaged shells. The red line represents the best-fit line that was used to impute the missing length measurements and all points with an imputed length also being colored red. The blue line represents the best-fit line that was used to impute the missing width measurements and all points with an imputed width also being colored red. Grey points were not missing any measurements.

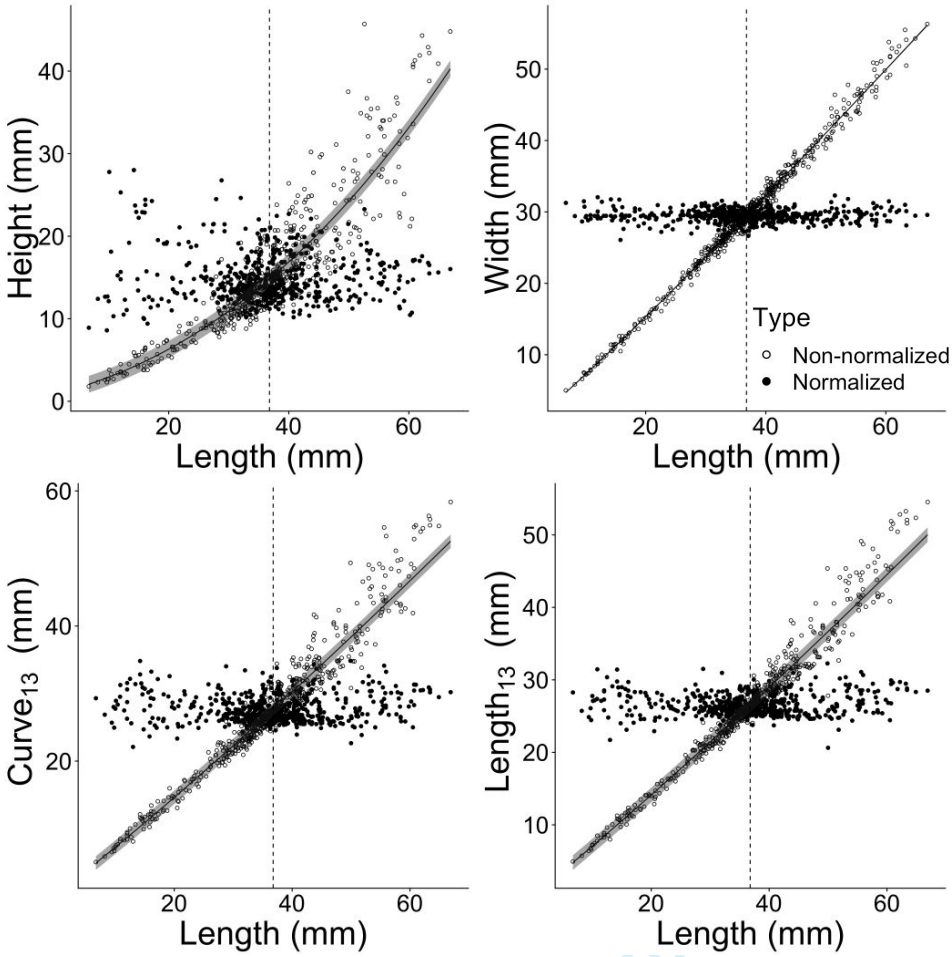

Figure S2. Scatter plots of shell (A) height, (B) width, (C) Curve1,3, and (D) Length 1,3) versus shell length before (lighter points, fit line) and after (darker points) normalization to subtract the effect of allometry from the measures. The dotted vertical line through the graphs represents the mean length around which the measurements were normalized (37 mm). The line through the pre-normalization points represents the best-fit model to the measurements which was used to normalize the points.

26